ELSEVIER

Neuroscience Letters 238 (1997) 29–32

Neuroscience Letters

Voltage signals of individual Purkinje cell dendrites in rat cerebellar slices

Alexander Borst*, Detlef Heck[1], Michael Thomann

Friedrich-Miescher-Laboratory of the Max Planck Society, Spemannstrasse 37–39, D-72076 Tuebingen, Germany

Received 9 July 1997; received in revised form 5 September 1997; accepted 3 November 1997

Abstract

For investigating neuronal information processing at the cellular level, a technique which visualizes the voltage distribution within single neurons in situ would be extremely useful. Voltage-sensitive dyes are, in principle, capable of reporting membrane potential [Cohen, L.B. and Salzberg, B.M., Rev. Physiol. Biochem. Pharmacol., 83 (1978) 35–88; Grinvald, A., Lieke, E.E., Frostig, R.D. and Hildesheim, R., J. Neurosci., 14 (1994) 2545–2568; Kleinfeld, D., Delaney, K.R., Fee, M.S., Flores, J.A., Tank, D.W. and Gelperin, A., J. Neurophysiol., 72 (1994) 1402–1419]. However, their application to single cells internally is technically difficult [Antic, S. and Zecevic, D., J. Neurosci., 15 (1995) 1392–1405; Grinvald, A., Salzberg, B.M., Lev-Ram, V. and Hildesheim, R., Biophys. J., 51 (1987) 643–651; Kogan, A., Ross, W.N., Zecevic, D. and Lasser-Ross, N., Brain Res., 700 (1995) 235–239; Zecevic, D., Nature, 381 (1996) 322–325]. An alternative strategy consists in applying the dye from the outside to all cells in the tissue, while manipulating a single cell by current injection [Krauthamer, V. and Ross, W.N., J. Neurosci., 4 (1984) 673–682; Ross, W.N. and Krauthamer, V., J. Neurosci., 4 (1984) 659–672]. Here, we modify this technique to further enhance spatial at the cost of temporal resolution [Borst, A., Z. Naturforsch., 50 (1995) 435–438]. Applied to rat cerebellar slices we demonstrate that the potential spread in individual Purkinje cells can be imaged up to even fine dendritic branches. The acquired optical signals suggest that steadily hyperpolarized Purkinje cells are electrically compact. When permanently depolarized, the somatic input resistance is significantly diminished, yet the spatial voltage drop along the dendrites remains unchanged. As demonstrated by compartmental modeling, this hints to a concentration of outward rectifying currents at the soma of the cells.

Keywords: Voltage-sensitive dye; Membrane potential; Optical recording; Imaging; Dendrite; Slice; Purkinje cell

To visualize the spatial steady-state voltage distribution within single Purkinje cells in situ we stained slices from young rats (p10–16) with a voltage-sensitive dye (Di8-ANEPPS; Molecular Probes) and measured the relative change of fluorescence ($\Delta F/F$) while a single Purkinje cell was stimulated periodically (Fig. 1a). To reveal the cell morphology, we added the fluorescent dye Cascade Blue (Molecular Probes) to the solution in the patch pipette (Fig. 1b). Cells had resting potentials between −50 and −70 mV, and input resistances ranged between 100 and 200 MΩ. Hyperpolarizing current pulses were injected periodically at a frequency of 0.66 Hz and, simultaneously, images were taken at the emission wavelength of Di8-ANEPPS (Fig. 1c). The time course of fluorescence at three different locations of the Di8 image stack revealed periodic increases of the optical signal during injection of hyperpolarizing current only in those locations where cellular processes were visible in the Cascade Blue image (Fig. 1d,e), but not elsewhere (Fig. 1f). To check for linearity of the optical signal with the membrane potential, different cells were hyper- and depolarized to various levels. The relative change of fluorescence varied with the membrane potential in a linear way, but differed from preparation to preparation (data not shown). On average, we obtained about 0.3% change of fluorescence per 100 mV (maximum value at the soma 2.0%/100 mV). However, the change in fluorescence also depends on factors other than the change

* Corresponding author. Tel.: +49 7071 601840; fax: +49 7071 601455; e-mail: alexander.borst@tuebingen.mpg.de

[1] Department of Neurobiology and Biophysics, University of Freiburg, D-79104 Freiburg, Germany.

0304-3940/97/$17.00
PII S0304-3940(97)00836-7

in membrane potential. Examples are (1) the amount of overlying tissue, (2) different staining intensity in different parts of the cell, or (3) the fact that parts of the cell are not perfectly focused. All these factors might contribute to some of the regional variations visible in the $\Delta F/F$ images shown in the following and restrict their immediate interpretation as voltage images. Therefore, an absolute calibration of a $\Delta F/F$ image in terms of membrane potential is not possible with this method, and any conclusion about the spatial voltage profile can only be drawn from many experiments. However, the method allows for a comparison of the electrical behavior of the same cell under different conditions

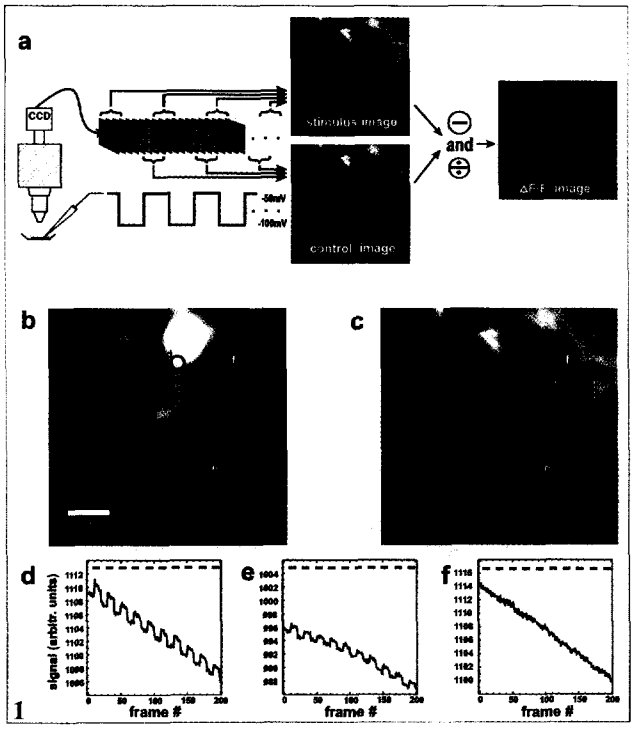

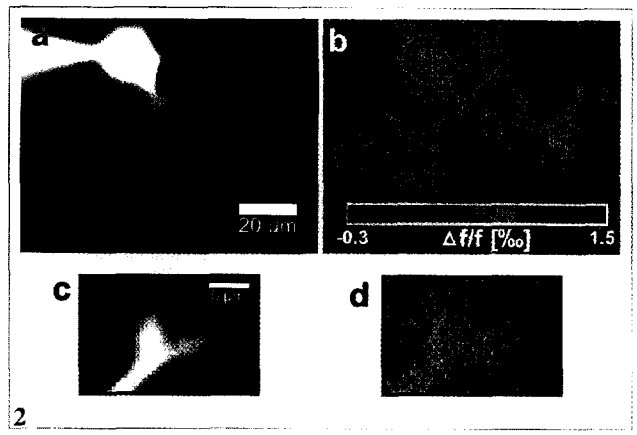

Fig. 1. (a) A Purkinje cell in the slice is periodically hyper- or depolarized while a series of images is taken. The $\Delta F/F$ image representing the relative difference between stimulus and control conditions leaves only the stimulated cell. (b,c) Fluorescence image of the slice at the excitation wavelength of the intracellular marker Cascade Blue (b) and of the voltage-sensitive dye (c). In (c), only the soma of cell is visible due to the staining of all other membranes in the molecular layer by extracellular application of the voltage-sensitive dye. Yet, not only at those parts of the image where the soma (d) but also where the dendrite (e) of the stimulated cell is located, the time course of the unprocessed fluorescence signal reveals periodic shifts in synchrony with the current pulses (indicated by blue bars) injected into the cell. In parts of the image where no cellular processes are located, no such modulation of the optical signal is visible (f). A fixed stage upright microscope (Axioskop FS with 63×, NA 0.9 water immersion objective; Zeiss) was equipped with epifluoresence illumination (XBO 75 xenon arc lamp) and the appropriate filter combinations. For voltage recording, we used the filter set #14 from Zeiss (BP 510–560, FT 580, LP 590). For the intracellular marker cascade blue, we used a filter set from Omega (BP 385–425, FT 450, LP 450). The microscope was furthermore equipped with IR-DIC optics and carried a beam splitter with an analog IR-sensitive video camera (C2400; Hamamatsu) for visual selection of the Purkinje cell on one end and a CCD camera (PXL, Photometrics, with a Kodak chip EEV, 512 × 512 pixels) connected to a computer (Power Mac 8100; Apple) for image acquisition on the other end. Slices were cut 300 μm thick from young rats (10–15 days old) using a vibroslice (752M; Campden Instruments). They were bathed at room temperature in ACSF containing 125 mM NaCl, 1 mM $MgCl_2$, 25 mM glucose, 2.5 mM KCl, 26 mM $NaHCO_3$, 1.25 mM NaH_2PO_4 and 2 mM $CaCl_2$. Patch pipettes had a resistance of about 3–4 MΩ. They were filled with a solution containing 140 mM KCl, 2 mM $MgCl_2$, 10 mM HEPES, 10 mM EGTA, 2 mM ATP and 0.5 mM Cascade Blue (Molecular Probes), adjusted to a pH of 7.3. Signals were recorded with an Axoclamp amplifier (Axon Instruments) operated in either current clamp or continuous voltage clamp mode. Observing an individual Purkinje cell under IR-DIC optics, slices were tilted around two orthogonal axes until the cell was aligned completely in the focal plane. The slice was subsequently stained for 5–10 min with the extracellular voltage-sensitive dye Di8-ANEPPS (Molecular Probes). After breaking into the cell in the whole-cell patch-clamp configuration, the cell was periodically hyper- or depolarized for 15 s (1.5 s cycle length, 50% duty-cycle). Within this sweep, 200 images (256 × 256 pixels) were taken by the CCD camera in frame-transfer mode at 13.3 Hz. The 200 images were then split in two parts, one half being those images taken while the cell was at rest (the control images C_i), the other half consisting of the images taken while the current was applied (the stimulus images S_i). These images were averaged separately. The final $\Delta F/F$ image was obtained by subtracting the averaged control image from the average stimulus image and dividing the result by the averaged control image: $\Delta F/F = (\Sigma S_i - \Sigma C_i)/\Sigma C_i$. Image processing was done using IPLab (Signal Analytics, Vienna, Austria).

Fig. 2. Anatomical image as revealed by injection of Cascade Blue (a) and false-color $\Delta F/F$ image (b) of a Purkinje cell with a hyperpolarizing current applied to the soma. During hyperpolarization of the soma by –50 mV from resting potential, no significant signal decay is detectable between the first order dendrite leaving the soma and dendritic tips. The areas indicated by a frame in (a) and (b) are shown enlarged in (c) and (d), respectively. Note the high resolution of the images with one pixel corresponding to 470 nm. The $\Delta F/F$ image represents the average obtained from four sweeps each comprising 100 stimulus and 100 control images.

(e.g. hyper- vs. depolarization) within a single experiment.

An example of a steady-state $\Delta F/F$ image of a Purkinje cell following hyperpolarizing current injection is shown in Fig. 2 (a, anatomy of the cell; b, $\Delta F/F$ image in false color code). The $\Delta F/F$ image (Fig. 2b) revealed almost all structures of the cell that were visible by the intracellular marker (compare with Fig. 2a). The enlarged areas of the images, shown in Fig. 2c,d, demonstrate the spatial resolution that was achieved under these conditions. In general, the signal was highest at the soma. Yet, this most likely does not reflect a larger somatic voltage than in the dendrite but rather the fact that, at the soma, overlaying tissue has been cleared away before establishing the whole cell configuration. Although the dendritic signal shows pronounced regional variation from pixel to pixel, we find that, on average, there was almost no decay of the $\Delta F/F$ signal within the dendrite up to the dendritic tips. Similar results were obtained in 11 other experiments. Thus, Purkinje cell dendrites seem to be electrically compact under steady-state hyperpolarizing conditions indicating a high specific membrane resistance all over the structure. While this has already been demonstrated for the main dendritic branches by dual electrode recordings [6], our results now suggest that it also holds true for the fine dendritic ramifications.

In order to investigate how the activation of voltage-gated ion channels affects the potential spread in Purkinje cells, we applied depolarizing current pulses to the soma. We compared four different stimulus situations: hyper- and

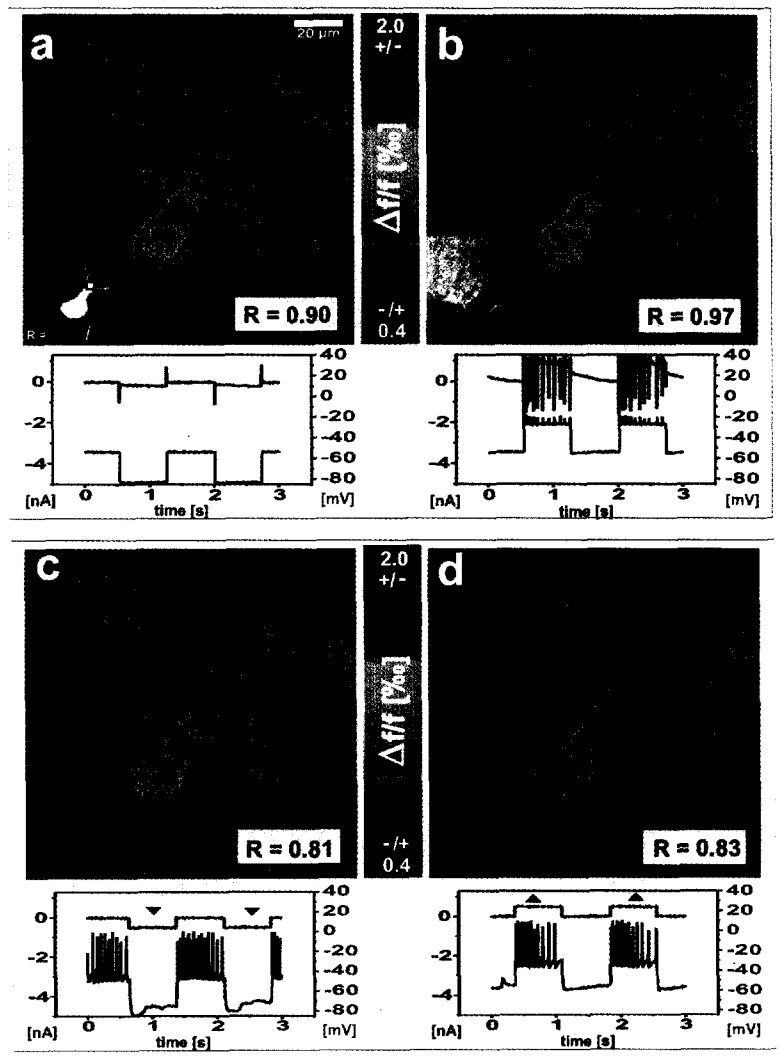

Fig. 3. (a–d) False-color $\Delta F/F$ images of a Purkinje cell which was periodically voltage-clamped at either −85 mV (a) or −25 mV (b), relative to a holding potential of −55 mV or was periodically hyperpolarized or depolarized under current clamp conditions by injection of −0.5 nA (c) or +0.5 nA (d), respectively. The color scale is inverted in the $\Delta F/F$ images under depolarizing conditions. Underneath each image, simultaneously recorded voltage and current signals are displayed. The inset in (a) shows the image of the same cell filled with Cascade Blue together with the areas which were used to calculate the signal attenuation along the dendrite in the four voltage images (R values). The inset in (b) shows the image of the Purkinje cell as observed with IR-DIC optics. Each $\Delta F/F$ image represents the average obtained from three sweeps each comprising 100 stimulus and 100 control images.

Table 1
Membrane parameters, somatic input resistance R_{IN} and voltage drop from proximal to distal dendrite in model Purkinje cells

	R_i (Ωcm)	$R_{m,soma}$ (Ωcm^2)	$R_{m,dend}$ (Ωcm^2)	R_{IN} (MΩ)	$\Delta V_{dist}/\Delta V_{prox}$ (%)
Control	225	760	45740	127	93
Condition 1: $R_{m,soma}$ reduced	225	335	45740	64	93
Condition 2: $R_{m,dend}$ reduced	225	760	4200	64	53
Condition 3: $R_{m,soma}$ and $R_{m,dend}$ reduced	225	667	4909	64	58

Purkinje cells from 12 day old rats were 3D-digitized after biocytin labeling [1] and modeled using the single cell simulator Nemosys [3]. R_i, specific internal resistivity; R_m, specific membrane resistance at the soma ($R_{m,soma}$) and in the dendrite ($R_{m,dend}$); ΔV_{dist}, ΔV_{prox}, voltage change in distal and proximal dendrite, respectively. Membrane parameters used for the control condition are taken from [5].

depolarizing voltage steps of 30 mV under voltage clamp conditions (Fig. 3a,b) and injection of 0.5 nA hyper- and depolarizing current pulses under current clamp conditions (Fig. 3c,d). When depolarized, the somatic input resistance dropped on average by about 33% ($n = 7$). The $\Delta F/F$ images as obtained under de- and hyperpolarizing voltage clamp conditions were almost identical (compare Fig. 3a and Fig. 3b). Under current clamp conditions, the $\Delta F/F$ image obtained for depolarization generally revealed weaker signals than for hyperpolarizing images due to the lower input resistance of the cell (compare Fig. 3c and Fig. 3d). To obtain a scalar measure for the voltage drop occurring along the dendrite under all conditions, we averaged the $\Delta F/F$ signals of a proximal and a distal dendritic region within each of the four images and calculated the ratio of these two values (see inset in Fig. 3a). The signal drop from the proximal to the distal dendrite amounted to the same value in all four cases (a–d). We therefore conclude that Purkinje cells do not change their electrotonic properties significantly during steady-state depolarization.

To study whether this finding hints to a particular spatial distribution of the currents responsible for the observed outward rectification during depolarization, we performed computer simulations using passive compartmental models of Purkinje cells obtained from rats of the same age as were used in the experiments. When the membrane parameters were set according to literature values of cells from adult animals [2,4,5], the somatic input resistance amounted to 127 MΩ and the steady-state voltage recorded at dendritic tips reached 93% of the value measured at the proximal dendrite. We then reduced the input resistance to 50% of its previous value in three different ways (Table 1): by decreasing the specific membrane resistance at the soma only (condition 1), exclusively in the dendrite (condition 2), or in both the soma and the dendrite by adding identical conductances (0.181 mS/cm^2) to both areas (condition 3). Only with a reduced membrane resistance at the soma did we observe an almost unchanged voltage spread within the dendrite. Otherwise, distal dendritic voltage signals reached only about 50% of the value as measured in the proximal dendrite. We conclude that the channels responsible for the reduced input resistance as measured under depolarizing conditions are concentrated at the soma of the cells and not spread over the dendrite. Consequently, the dendritic membrane resistance remains unchanged in all dendritic ramifications during depolarization. This result is of particular functional importance when the signal spread from the dendrite to the soma of Purkinje cells is considered, e.g. for parallel fiber input [2].

We are grateful to B. Antkowiak for useful advice, to H. Nguyen and B. Bochenek for excellent technical assistance and to R. Friedrich, J. Haag and T. Oertner for critically reading the manuscript.

[1] Borst, A. and Haag, J., The intrinsic electrophysiological characteristics of fly lobula plate tangential cells. I. Passive membrane properties, J. Comput. Neurosci., 3 (1996) 313–336.
[2] de Schutter, E. and Bower, J.M., An active membrane model of the cerebellar Purkinje cell. I. Simulation of current clamps in slice, J. Neurophysiol., 71 (1994) 375–400.
[3] Eeckman, F.H., Theunissen, F.E. and Miller, J.P., Nemosys: a system for realistic single neuron modeling. In J. Skrzypek (Ed.), Neural Network Simulation Environments, Kluwer Academic, Dordrecht, 1994, pp. 114–135.
[4] Rapp, M., Segev, I. and Yarom, Y., Physiology, morphology and detailed passive models of guinea-pig cerebellar Purkinje cells, J. Physiol., 474.1 (1994) 101–118.
[5] Shelton, D.P., Membrane resistivity estimated for the Purkinje neuron by means of a passive computer model, Neuroscience, 14 (1985) 111–131.
[6] Stuart, G. and Häusser, M., Initiation and spread of sodium action potentials in cerebellar Purkinje cells, Neuron, 13 (1994) 703–712.